

## Kinetics of degradation in aqueous solution of Abbott-79175, a potent second generation 5-lipoxygenase inhibitor

Jay S. Trivedi, James J. Fort \*

*D-493 Pharmaceutics Department, Pharmaceutical Products Division, Abbott Laboratories, Abbott Park, IL 60064–3500, USA*

Received 22 December 1993; revised 27 October 1994; accepted 2 February 1995

### Abstract

The degradation kinetics of Abbott-79175 in aqueous solution have been studied as a function of pH. Concentration/time plots indicated a pseudo-first order nature of reactions throughout the pH range studied. Additionally, the effects of temperature, ionic strength, and buffer concentration have been examined. From multiple temperature experiments, Arrhenius and activation parameters were calculated. Furthermore, it was determined that upon ionization, Abbott-79175 degradation proceeded independently of ionic strength. These data in addition to the plateau-like nature of the pH-rate constant profile above pH 10 suggest a lack of participation of hydroxide ion during the reaction. This behavior in the neutral and alkaline regions was qualitatively very similar to that of zileuton, a 5-lipoxygenase inhibitor in phase III clinical trials. In addition to allowing the determination of the buffer independent rate constants, kinetic studies as a function of buffer concentration allowed in some of the systems the deduction of which buffer species were catalytic. A multi-parameter model was fitted to the pH buffer independent rate constant data using non-linear regression. This modeling yielded parameters such as the microscopic rate constants and the  $pK_a$  under the aforementioned conditions. From the pH-rate constant profile, Abbott-79175 was found to be more labile than zileuton throughout the pH range studied. This difference was greater than three orders of magnitude at pH 1. Such acid lability produced a pH profile which had a much narrower region of maximum stability.

*Keywords:* 5-Lipoxygenase; Hydroxyurea; Kinetics; Buffer catalysis; Ionic strength effect; Temperature effect

### 1. Introduction

Inflammatory disorders such as arthritis, asthma, ulcerative colitis, rhinitis, and psoriasis are presently treated with a variety of therapeutic agents such as steroids and cytostatic agents, as well as the non-steroidal anti-inflammatory agents

(NSAIDs) (Flower et al., 1985). Numerous NSAIDs can be found on the prescription and non-prescription market. These agents as a class generally inhibit one cyclooxygenase (or prostaglandin synthetase) which is responsible for the conversion of arachidonic acid to various prostaglandins (Flower et al., 1985; Moncada et al., 1985). In addition to being a precursor to prostaglandins, arachidonate is also the precursor to leukotrienes (often called the slow reacting

\* Corresponding author.

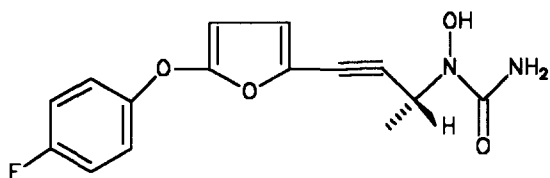


Fig. 1. Chemical structure of Abbott-79175. Chemical name: *R*-(+)-*N*-[3-[5-(fluorophenoxy)-2-furanyl]-1-methyl-2-propynyl]-*N*-hydroxyurea. Molecular formula:  $C_{15}H_{13}FN_2O_4$  Molecular weight: 304.28.

substance of anaphylaxis), in this case the converting enzyme being 5-lipoxygenase (5-LO). Leukotrienes produce smooth muscle contraction, cause increases in vascular permeability, and are potent chemotactic substances (Wasserman et al., 1991). Inhibition of 5-LO represents another strategy for the treatment of many inflammatory disorders by the reduction of the levels of leukotrienes, which are potent inflammatory mediators.

One agent in the hydroxyurea class of 5-LO inhibitors is zileuton (Abbott-64077) (Brooks et al., 1990; Carter et al., 1991) which is currently in clinical trials for the treatment of asthma. The stability of this compound in aqueous solution, along with the characterization of its degradation pathway, has been elegantly described (Alvarez and Slade, 1992). The mechanism of degradation of this compound was shown to be hydrolysis at the amide functionality producing the corresponding hydroxylamine and carbamic acid as primary degradation products.

The current study examines the solution stability kinetics of a new 5-LO inhibitor, Abbott-79175 (Fig. 1). The biological properties of the racemic mixture of this compound and its enantiomer have been described (Bell et al., 1993).

## 2. Materials and methods

### 2.1. Materials

Abbott-79175 (lot 58-190-AL) was generously provided by the immunoscience venture at Abbott Laboratories. Water utilized in the study was

HPLC grade (EM science) and all other solvents utilized were of HPLC grade. All other materials were analytical reagent grade.

### 2.2. HPLC assay

Abbott-79175 was quantitated by high-performance liquid chromatography (HPLC). The HPLC system consisted of a Hitachi AS4000 Autosampler equipped with a 100  $\mu$ l loop, a Spectra Physics SP8800 ternary pump, Kratos Spectroflow 783 variable-wavelength detector and Spectra Physics 4270 Integrator. The column was a Regis Octadecyl Workhorse 30 cm  $\times$  4.6 mm i.d. code 731118. The mobile phase was 50:50 (0.1% v/v perchloric acid with 0.025% w/v acetohydroxamic acid)/acetonitrile, with a 2 ml/min flow rate. The wavelength of detection was 264 nm, with a typical injection volume of 100  $\mu$ l. The analyte was quantitated from linear standard curves of peak area obtained from the integrator vs concentration. The drug peak was shown to be clearly resolved from degradation products in all studies where such interference was a possibility.

### 2.3. $pK_a$ estimation

The solubility method for  $pK_a^*$  (estimate) determination was performed for Abbott-79175. Solubilities at 40°C were determined in triplicate from pH 7.50 to 11.72. The buffers utilized were 0.05 M and  $\mu = 0.5$ . Sodium phosphate was employed for pH 7.47–8.49, 11.45, and 11.96, while sodium carbonate was used for pH 9.00–11.01. Sodium chloride was the ionic strength adjuster. 0.5–1 mg quantities of drug were placed in 0.6 ml of buffer solution and were allowed to equilibrate for 72 h in a rotating bath apparatus (20 rpm). At the end of the equilibration period, the samples were removed from the bath, immediately filtered through a 0.45  $\mu$ m filter (Acrodisc 3 cr PTFE) attached to a disposable syringe (Bectin-Dickinson). It was confirmed at as low a concentration as  $\sim 7$   $\mu$ g/ml that filtration did not cause an underestimation of drug concentration due to filter adsorption. The filtrate was then immediately diluted with acetonitrile/water (50:50) and injected into the HPLC apparatus. The pH was

obtained from the combined remaining filtrates of the three replicates immediately after the aliquots were removed for dilution.

#### 2.4. Aqueous solution kinetic studies

Solution kinetic studies were performed by preparing a stock solution of Abbott-79175 in methanol ( $\sim 1300 \mu\text{g/ml}$ ) and diluting this with the reaction medium (1:100 dilution) to arrive at a final drug concentration of  $\sim 13 \mu\text{g/ml}$ . Most studies were performed by placing aliquots of this reaction medium into 2 ml ampules which were then sealed and placed in the appropriate oven (40, 60, 70°C). The degradation studies under more accelerated reaction conditions were performed by adding the drug dissolved in methanol to a scintillation vial containing the pre-heated reaction medium. The samples were then taken with a micro-pipette and diluted with a quenching medium (chilled 50:50 acetonitrile/water). These samples were then immediately loaded onto the autosampler which was equipped with a chilled ( $\sim 10^\circ\text{C}$ ) tray.

The pH values examined in this study (1–13) were maintained by buffer species having a  $pK_a$  within 1.5 pH units of the desired pH, with the exceptions of 1 and 13 which were 0.1 N HCl and NaOH, respectively. Sodium phosphate was utilized in pH 2, 3, 6, 7, 8, and 12 systems, sodium acetate at pH 4 and 5, and sodium carbonate at pH 9.2, 10, and 11. Actual pH values for each study will be listed with the appropriate kinetic data. When pH values are not specified to two decimal places, they were within 0.1 units of the target value. Typically, multiple buffer concentrations were studied at a particular pH so as to allow the calculation of the buffer independent rate constant. Usually, 0.05, 0.10, 0.15, and 0.2 M buffer concentrations were used, however, in the higher pH regions (phosphate buffer), 0.05, 0.075, 0.1, and 0.125 M concentrations were utilized. In these experiments, the ionic strength was maintained at  $0.5 (\pm 0.02)$ . Four exceptions were the pH 12 buffers of 0.05, 0.075, and 0.1 M, that were  $\mu = 0.531, 0.530,$  and  $0.588,$  respectively, and the 0.2 M pH 8 buffer with  $\mu = 0.582$ . Buffer calculations involved the use of the Davies expression

for activity coefficient calculations (Davies, 1962) and were performed on Equil v. 2.13 (MicroMath Scientific Software). The effect of ionic strength was studied in the alkaline pH range (pH 13). The ionic strengths used were 0.1–0.5 at 0.1 increments. Temperatures of all studies were monitored using regularly calibrated thermometers. Oven and bath temperatures were maintained at  $\pm 1^\circ\text{C}$ .

### 3. Results and discussion

#### 3.1. Observed kinetic order

Previous work (Alvarez and Slade, 1992) on the stability of zileuton demonstrated degradation kinetics that were pseudo-first order in nature. The pH-rate profile for zileuton showed a direct dependence of the rate constant on the proton concentration in the acidic range, a pH independent rate constant between pH 3 and 8, and dependence on the degree of ionization of zileuton around the  $pK_a$  with pH independence of the rate constant at pH values above 10. Representative concentration vs time plots for two extreme pH values for Abbott-79175 are shown in Fig. 2. The kinetics appeared to be pseudo-first order at all pH values studied.

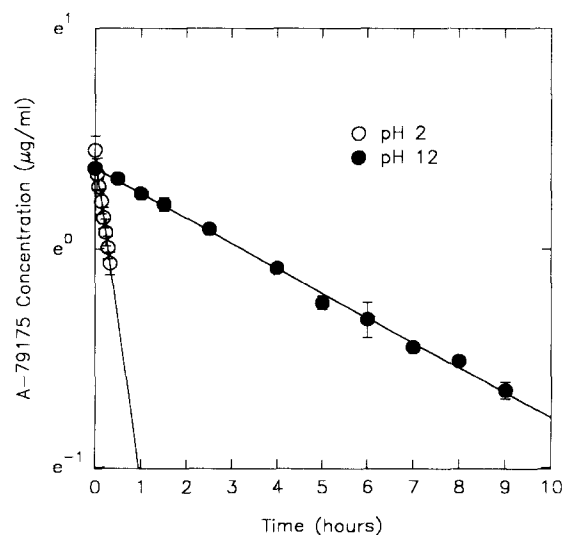


Fig. 2. Concentration vs time profile for Abbott-79175 in aqueous solution at  $40^\circ\text{C}$  at two pH extremes.

Table 1  
Effect of pH and buffer concentration on rate of Abbott-79175 degradation at 40°C

pH	Buffer concentration (M)					
	0.05	0.075	0.10	0.125	0.15	0.20
2.05	1.49 <sup>a</sup>		2.40		3.15	3.81
3.06	0.18		0.22		0.29	0.41
3.99	0.028		0.040		0.051	0.055
4.99	0.007		0.012		0.018	0.021
6.00	0.006		0.009		0.012	0.015
7.03	0.0051		0.0055		0.0065	0.0079
8 <sup>b</sup>	0.005		0.007	0.007	0.008	
9.22	0.016		0.019		0.019	0.019
10 <sup>b</sup>	0.103		0.051		0.093	0.076
11.00	0.11	0.11	0.15		0.13	
12.01	0.11	0.15	0.16			

<sup>a</sup> All rate constants are expressed in h<sup>-1</sup>.

<sup>b</sup> pH within 0.1 units of target value.

### 3.2. General acid / base catalysis

The effects of buffer concentration on the rate of degradation of Abbott-79175 for various buffers are listed in Table 1, with an example plot shown in Fig. 3. The buffers employed in this study were sodium phosphate, acetate and carbonate. In order to understand the contribution of each species for a particular buffer, where possible, their

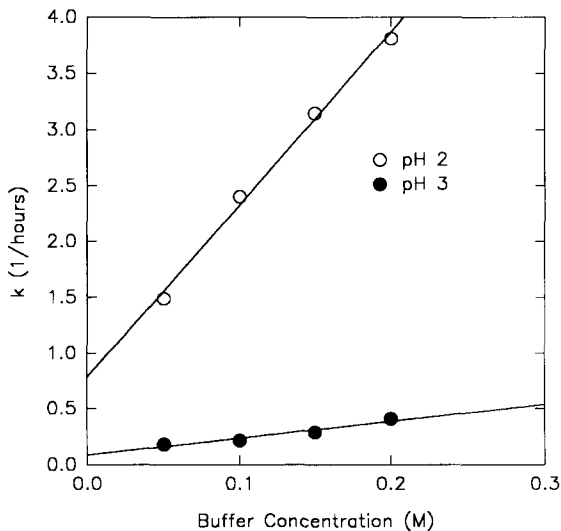


Fig. 3. Plot of observed rate constant vs phosphate buffer concentration at 40°C and  $\mu = 0.5$ .

macro-catalytic rate constants were calculated from rate vs buffer concentration data. Then, considering the individual species concentrations, and these macro-constants as a function of pH, the probable catalytic species were deduced in most pH regions. Equations from which species concentrations at various pH values can be calculated are shown below:

For phosphate:

$$K_1 = \frac{a_{H^+}[H_2PO_4^-]\gamma_-}{[H_3PO_4]} \quad (1)$$

$$K_2 = \frac{a_{H^+}[HPO_4^{2-}]\gamma_{2-}}{[H_2PO_4^-]\gamma_-} \quad (2)$$

$$K_3 = \frac{a_{H^+}[PO_4^{3-}]\gamma_{3-}}{[HPO_4^{2-}]\gamma_{2-}} \quad (3)$$

where  $a_{H^+}$  is the proton activity, and the  $\gamma_-$ ,  $\gamma_{2-}$ , and  $\gamma_{3-}$  denote the activity coefficients for the ionized phosphate species with their corresponding signs. The catalytic components of the various phosphate species are described below.

$$k_{obs} = k_0 + k_{phosphate}[\text{phosphate}] \quad (4a)$$

$$= k_0 + k_{H_3PO_4}[H_3PO_4] + k_{H_2PO_4^-}[H_2PO_4^-] + k_{HPO_4^{2-}}[HPO_4^{2-}] + k_{PO_4^{3-}}[PO_4^{3-}] \quad (4b)$$

$$= k_0 + k_{H_3PO_4}f_{H_3PO_4}[\text{phosphate}] + k_{H_2PO_4^-}f_{H_2PO_4^-}[\text{phosphate}] + k_{HPO_4^{2-}}f_{HPO_4^{2-}}[\text{phosphate}] + k_{PO_4^{3-}}f_{PO_4^{3-}}[\text{phosphate}] \quad (4c)$$

where  $f$  values are concentration fractions of the various phosphate species. Following from above, these fractions are represented below:

$$f_{H_3PO_4} = \frac{a_{H^+}^3}{a_{H^+}^3 + a_{H^+}^2K_1/\gamma_- + a_{H^+}K_1K_2/\gamma_{2-} + K_1K_2K_3/\gamma_{3-}} \quad (4d)$$

$$f_{H_2PO_4^-} = \frac{a_{H^+}^2K_1/\gamma_-}{a_{H^+}^3 + a_{H^+}^2K_1/\gamma_- + a_{H^+}K_1K_2/\gamma_{2-} + K_1K_2K_3/\gamma_{3-}} \quad (4e)$$

$$f_{\text{HPO}_4^{2-}} = \frac{a_{\text{H}^+} K_1 K_2 / \gamma_{2-}}{a_{\text{H}^+}^3 + a_{\text{H}^+}^2 K_1 / \gamma_{-} + a_{\text{H}^+} K_1 K_2 / \gamma_{2-} + K_1 K_2 K_3 / \gamma_{3-}} \quad (4f)$$

$$f_{\text{PO}_4^{3-}} = \frac{K_1 K_2 K_3 / \gamma_{3-}}{a_{\text{H}^+}^3 + a_{\text{H}^+}^2 K_1 / \gamma_{-} + a_{\text{H}^+} K_1 K_2 / \gamma_{2-} + K_1 K_2 K_3 / \gamma_{3-}} \quad (4g)$$

For the pH 2 and 3 systems, it can be discerned from the observed catalytic constants (slope of observed rate constant vs buffer concentration) and the relative species percentages (see Table 2) that H<sub>3</sub>PO<sub>4</sub> is the most catalytic of the two species. In the pH 6–7 range, the data in Table 2 suggest that the H<sub>2</sub>PO<sub>4</sub><sup>-</sup> species is most catalytic since the highest catalytic constant is associated with the greatest proportion of H<sub>2</sub>PO<sub>4</sub><sup>-</sup>.

For acetate, an analogous, although more simplified, treatment is shown below:

$$K_1 = \frac{a_{\text{H}^+} [\text{OAc}^-] \gamma_{-}}{[\text{HOAc}]} \quad (5)$$

a<sub>H<sup>+</sup></sub> represents proton activity as before, and γ<sub>-</sub> denotes the acetate ion activity coefficient. The expression for catalytic micro-constants is derived below.

$$k_{\text{obs}} = k_0 + k_{\text{acetate}} [\text{acetate}] \quad (6a)$$

$$= k_0 + k_{\text{HOAc}} [\text{HOAc}] + k_{\text{OAc}^-} [\text{OAc}^-] \quad (6b)$$

$$= k_0 + k_{\text{HOAc}} f_{\text{HOAc}} [\text{acetate}] + k_{\text{OAc}^-} f_{\text{OAc}^-} [\text{acetate}] \quad (6c)$$

The species fractions are shown below:

$$f_{\text{HOAc}} = \frac{a_{\text{H}^+}}{a_{\text{H}^+} + K_1 / \gamma_{-}} \quad (6d)$$

$$f_{\text{OAc}^-} = \frac{K_1 / \gamma_{-}}{a_{\text{H}^+} + K_1 / \gamma_{-}} \quad (6e)$$

One additional consideration in the case of sodium acetate is the association of sodium and acetate ions in an ion pair. Such association has been shown experimentally (Archer and Monk, 1964). The contribution of this ion pair species is ~ 3% at pH 4 and ~ 10% at pH 5. The catalytic contribution of this species is assumed to be relatively small especially in light of the other two potentially catalytic species. This assumption is made since, due to ionic association, there is no available nucleophile (carboxylate anion) for a catalytic effect.

At pH 4 and 5, from an examination of the relative magnitude of the catalytic constants at these pH values, the acidic component of the buffer (HOAc) is suggested to be more catalytic than its conjugate base (OAc<sup>-</sup> or NaOAc for that matter), since the overall catalytic constant increased substantially along with an increase in the HOAc percentage.

For carbonate, once more an analogous treatment to those with the two other buffer system applies:

$$K_1 = \frac{a_{\text{H}^+} [\text{HCO}_3^-] \gamma_{-}}{[\text{H}_2\text{CO}_3]} \quad (7)$$

Table 2  
Catalytic macro-constants and species concentrations for low and high buffer concentrations vs pH

pH	k <sub>cat</sub> <sup>b</sup> (l/mol per h)	Species (%)	
		Low concentration <sup>a</sup>	High concentration <sup>a</sup>
2	15.42	50.52 H <sub>3</sub> PO <sub>4</sub> , 49.48 H <sub>2</sub> PO <sub>4</sub> <sup>-</sup>	50.54 H <sub>3</sub> PO <sub>4</sub> , 49.49 HPO <sub>4</sub> <sup>-</sup>
3	1.496	9.07 H <sub>3</sub> PO <sub>4</sub> , 90.91 H <sub>2</sub> PO <sub>4</sub> <sup>-</sup>	9.07 H <sub>3</sub> PO <sub>4</sub> , 90.90 HPO <sub>4</sub> <sup>-</sup>
4	0.184	78.08 HOAc 18.99 OAc <sup>-</sup> , 2.93 NaOAc	78.08 HOAc 18.99 OAc <sup>-</sup> , 2.92 NaOAc
5	0.096	26.27 HOAc 63.88 OAc <sup>-</sup> , 9.86 NaOAc	26.28 HOAc 63.90 OAc <sup>-</sup> , 9.83 NaOAc
6	0.06	82.95 H <sub>2</sub> PO <sub>4</sub> <sup>-</sup> , 7.05 HPO <sub>4</sub> <sup>2-</sup>	82.96 H <sub>2</sub> PO <sub>4</sub> <sup>-</sup> , 17.04 HPO <sub>4</sub> <sup>2-</sup>
7	0.019	31.23 H <sub>2</sub> PO <sub>4</sub> <sup>-</sup> , 68.76 HPO <sub>4</sub> <sup>2-</sup>	31.26 H <sub>2</sub> PO <sub>4</sub> <sup>-</sup> , 68.74 HPO <sub>4</sub> <sup>2-</sup>
8	0.028	4.64 H <sub>2</sub> PO <sub>4</sub> <sup>-</sup> , 95.32 HPO <sub>4</sub> <sup>2-</sup>	4.64 H <sub>2</sub> PO <sub>4</sub> <sup>-</sup> , 95.32 HPO <sub>4</sub> <sup>2-</sup>
9.2	0.017	76.2 HCO <sub>3</sub> <sup>-</sup> , 23.8 CO <sub>3</sub> <sup>2-</sup>	76.2 HCO <sub>3</sub> <sup>-</sup> , 23.8 CO <sub>3</sub> <sup>2-</sup>
10	-0.078	34.7 HCO <sub>3</sub> <sup>-</sup> , 65.3 CO <sub>3</sub> <sup>2-</sup>	34.6 HCO <sub>3</sub> <sup>-</sup> , 65.4 CO <sub>3</sub> <sup>2-</sup>
11	0.287	5 HCO <sub>3</sub> <sup>-</sup> , 95 CO <sub>3</sub> <sup>2-</sup>	5 HCO <sub>3</sub> <sup>-</sup> , 95 CO <sub>3</sub> <sup>2-</sup>
12	0.96	18.37 HPO <sub>4</sub> <sup>2-</sup> , 81.63 PO <sub>4</sub> <sup>3-</sup>	18.27 HPO <sub>4</sub> <sup>2-</sup> , 81.73 PO <sub>4</sub> <sup>3-</sup>

<sup>a</sup> Lowest and highest buffer concentrations used for a given pH.

<sup>b</sup> Obtained from k<sub>obs</sub> vs buffer concentration plots (data in Table 1).

$$K_2 = \frac{a_{\text{H}^+} [\text{CO}_3^{2-}] \gamma_{2-}}{[\text{HCO}_3^-] \gamma_-} \quad (8)$$

$$k_{\text{obs}} = k_0 + k_{\text{carbonate}} [\text{carbonate}] \quad (9a)$$

$$= k_0 + k_{\text{H}_2\text{CO}_3} [\text{H}_2\text{CO}_3] + k_{\text{HCO}_3^-} [\text{HCO}_3^-] + k_{\text{CO}_3^{2-}} [\text{CO}_3^{2-}] \quad (9b)$$

$$k_{\text{obs}} = k_0 + k_{\text{H}_2\text{CO}_3} f_{\text{H}_2\text{CO}_3} [\text{carbonate}] + k_{\text{HCO}_3^-} f_{\text{HCO}_3^-} [\text{carbonate}] + k_{\text{CO}_3^{2-}} f_{\text{CO}_3^{2-}} [\text{carbonate}] \quad (9c)$$

In the pH range this buffer system was utilized, where the carbonic acid concentration is miniscule; the species fractions are:

$$f_{\text{HCO}_3^-} = \frac{a_{\text{H}^+}}{a_{\text{H}^+} + K_2 \gamma_- / \gamma_{2-}} \quad (9d)$$

$$f_{\text{CO}_3^{2-}} = \frac{K_2 \gamma_- / \gamma_{2-}}{a_{\text{H}^+} + K_2 \gamma_- / \gamma_{2-}} \quad (9e)$$

An assessment of which carbonate buffer component is most operative in a catalytic sense is more difficult to make. The carbonate buffer is utilized in the pH range over which Abbott-79175 undergoes ionization. Therefore, more than just the relative buffer species proportions change over this range. While the catalytic constant at pH 11 is considerably larger than those at either 9.2 or 10 (Table 2), it is very difficult to draw any inference from the data with a high level of confidence, except that 95% of the concentration of the buffer at this pH is the doubly anionic carbonate species. As a result, the concentration of bicarbonate very low and less likely to be the catalyst.

### 3.3. pH-rate profile

The log degradation rate constant vs pH profile at 40°C is shown in Fig. 4. The data points on this plot represent the rate constants at zero buffer concentration ( $k_0$ ) obtained from plots of  $k_{\text{obs}}$  vs buffer concentration, while the curve through the data points represents the non-linear fit of the data to the mathematical model developed in the following discussion. The possible

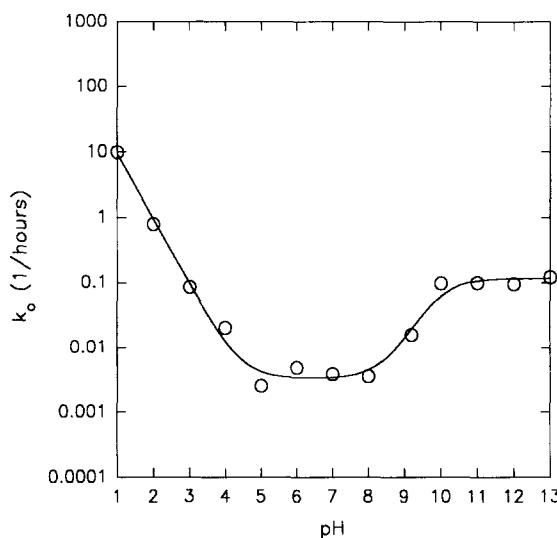


Fig. 4. Plot of buffer independent rate constant vs pH for Abbott-79175 at 40°C and  $\mu = 0.5$ .

reactions of Abbott-79175 in aqueous solution to products (P) are shown below:

Reaction	Rate constant
$\text{DH} + \text{H}^+ \xrightarrow{\text{H}_2\text{O}} \text{P}$	$k_1$
$\text{DH} \xrightarrow{\text{H}_2\text{O}} \text{P}$	$k_2$
$\text{DH} + \text{OH}^- \xrightarrow{\text{H}_2\text{O}} \text{P}$	$k_3$
$\text{D}^- \xrightarrow{\text{H}_2\text{O}} \text{P}$	$k_4$
$\text{D}^- + \text{OH}^- \xrightarrow{\text{H}_2\text{O}} \text{P}$	$k_5$

$$v = -d[\text{D}]/dt$$

$$= k_{\text{obs}}[\text{D}] = k_1[\text{DH}][\text{H}^+] + k_2[\text{DH}] + k_3[\text{DH}][\text{OH}^-] + k_4[\text{D}^-] + k_5[\text{D}^-][\text{OH}^-] \quad (10)$$

where  $v$  is the velocity of the reaction,  $[\text{D}]$  the total concentration of Abbott-79175 in solution,  $[\text{DH}]$  the concentration of undissociated Abbott-79175, and  $[\text{D}^-]$  the concentration of Abbott-79175 anion produced by deprotonation at the hydroxyurea -OH functionality.  $k_1$ – $k_5$  are the

microscopic rate constants for the various reactions.

$$[D] = [DH] + [D^-] \quad (11)$$

with

$$K_a = \frac{a_{H^+}[D^-]\gamma_{D^-}}{[DH]} \quad (12)$$

where  $a_{H^+}$  and  $\gamma_{D^-}$  are the hydrogen ion activity and activity coefficient of ionized drug, respectively, while  $K_a$  denotes the ionization constant of the drug.

$$f_{DH} = \frac{[DH]}{[DH] + [D^-]} \quad (13a)$$

and

$$f_{D^-} = \frac{[D^-]}{[DH] + [D^-]} \quad (14a)$$

combining the above:

$$f_{DH} = \frac{a_{H^+}}{a_{H^+} + K_a/\gamma_{D^-}} \quad (13b)$$

and

$$f_{D^-} = \frac{K_a/\gamma_{D^-}}{a_{H^+} + K_a/\gamma_{D^-}} \quad (14b)$$

Consequently:

$$k_{obs} = \{k_1 a_{H^+}^2/\gamma_{H^+} + k_2 a_{H^+} + k_3 K_w/\gamma_{OH^-} + k_4 K_a/\gamma_{D^-} + k_5 K_a K_w/a_{H^+}\gamma_{D^-}\gamma_{OH^-}\} \times \{a_{H^+} + K_a/\gamma_{D^-}\}^{-1} \quad (15a)$$

where  $K_w$  is the autoprotolysis constant of water and  $\gamma_{OH^-}$  represents the activity coefficient of hydroxide ion.

The general shape of the log degradation rate constant vs pH profile demonstrates that Abbott-79175 has considerable lability to acid catalysis (Fig. 4). Abbott-79175 shows a profile which is virtually unaffected by base, but is dependent on the degree of ionization of the molecule, which reacts directly with the solvent.

Upon ionization of Abbott-79175 the rate ceases to increase, with the explanation in electrostatic terms that this negatively charged molecule will not be susceptible to attack by the

$OH^-$  nucleophile at the amide bond. The most likely scenario is that the attacking species in hydrolysis is water, which would explain the lack of dependency on the  $OH^-$  concentration. In addition to the pH independence of the profile in the alkaline region, the potential reaction of a negatively charged hydroxide ion attacking the Abbott-79175 anion is unlikely in light of results from rate vs ionic strength experiments, which show no discernible effect of ionic strength on the reaction rate constant. This lack of effect of ionic strength on rate is discussed in section 3.4.

From the observed pH-rate data, there is definitely a dependence on the proton concentration, a plateau region from approx. pH 5–8, and a definite pH independence above the apparent  $pK_a$  of the molecule. The pH independence in this region eliminates the need for a term containing  $k_5$ . It was also determined by a non-linear fit of an equation containing five parameters ( $k_1$ – $k_4$ , and the  $pK_a$ ) that the values for  $k_1$ ,  $k_2$ , and  $k_4$  and the  $pK_a$  were similar with or without the term containing  $k_3$ . From this observation, a four-parameter model was deemed the most appropriate one. This model, which was simplified from Eq. 15a, is shown below.

$$k_{obs} = \frac{k_1 a_{H^+}^2/\gamma_{H^+} + k_2 a_{H^+} + k_4 K_a/\gamma_{D^-}}{a_{H^+} + K_a/\gamma_{D^-}} \quad (15b)$$

The elimination of rate constants  $k_3$  and  $k_5$  emphasizes the lack of contribution of hydroxide ion catalysis in the degradation of Abbott-79175. The microscopic rate constants and the  $pK_a$  obtained from a non-linear fit of this model to the experimental data are shown in Table 3.

The following model was fitted to the experimental solubility data for Abbott-79175 for the

Table 3

Microscopic rate constants obtained from non-linear regression using kinetic model at 40°C<sup>a</sup>

$k_1$ (l/mol per h)	$k_2$ (h <sup>-1</sup> )	$k_4$ (h <sup>-1</sup> )	$pK_a$
64.2 (11.7) <sup>a</sup>	0.0033 (0.0007)	0.1164 (0.0234)	10.14 (0.22)

<sup>a</sup> Monovalent activity coefficient of 0.684 utilized in fitting Eq. 15b.

<sup>b</sup> Standard error of parameter,  $r = 0.992$ .

Table 4  
Solubility of Abbott-79175 at 40° C as a function of pH

pH <sup>a</sup>	Apparent solubility <sup>b</sup> ( $\mu\text{g/ml}$ )
7.50	21.0 (0.3)
8.02	20.0 (0.1)
8.38	20.4 (0.5)
9.05	22.9 (0.5)
9.60	25.4 (0.1)
9.94	26.3 (1.0) <sup>c</sup>
10.44	55.2 (3.0)
10.70	70.1 (1.8)
11.34	240.6 (10.7) <sup>c</sup>
11.72	492.2 (1.1)

<sup>a</sup> pH values after equilibration as described in text.

<sup>b</sup> Solubilities are averages of three replicates with standard error of mean (SE) in parentheses.

<sup>c</sup> Average and SE from two replicates.

purpose of estimating the  $pK_a$  independently (Table 4).

$$S_{\text{obs}} = S_{\text{HB}}[10^{(\text{pH} - pK_a^*)}] + S_{\text{HB}} \quad (16)$$

$S_{\text{obs}}$  represents the observed solubility at 40° C, and  $S_{\text{HB}}$  the intrinsic solubility of Abbott-79175 at this temperature. From a non-linear fit (Fig. 5) to the Abbott-79175 solubility data, a  $pK_a^*$  of 10.33 (with a standard error of 0.02) and an intrinsic solubility of 20.7  $\mu\text{g/ml}$  (standard error of 0.4  $\mu\text{g/ml}$ ) were obtained. This  $pK_a^*$  value is

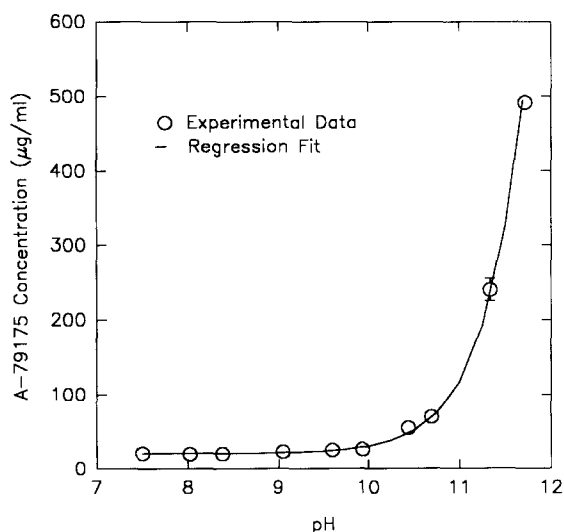


Fig. 5. Abbott-79175 solubility as a function of pH at 40° C in 0.05 M buffers ( $\mu = 0.5$ ).

an estimate and not considered a thermodynamic value. This is the case because the concentrations of drug, particularly under conditions where it is ionized, are large and contribute to the ionic strength of the medium. Furthermore, some unavoidable degradation occurred in the medium which also has an influence on the ionic environment. Although not a thermodynamic  $pK_a$ , it does serve as the best independent estimate method available (this is the case since titrimetric and spectrophotometric methods were not applicable to this compound). Although this  $pK_a$  and the one obtained from the kinetic analysis (10.14) are reasonably close considering the experimental error from the stability-derived number, any difference observed between the two values can largely be attributed to buffer effects (which were negated in the kinetic analysis) and effects of drug degradation on the nature of the solubilization medium.

When the profile is compared to that for zileuton, it is shown that Abbott-79175 is considerably more labile, particularly in the acidic range (Fig. 6). The zileuton data at 40° C and 0.05 M were calculated from data originally reported by Alvarez and Slade (1992). The ionic strength in the

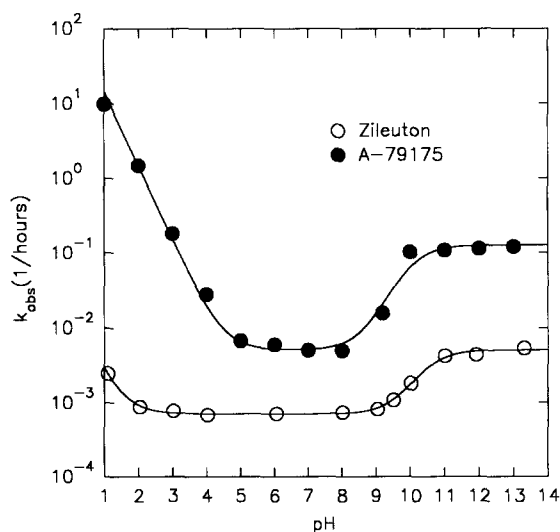


Fig. 6. Comparison of observed rate constant vs pH for Abbott-79175 and zileuton at 0.05 M buffer concentration and  $\mu = 0.5$  at 40° C.



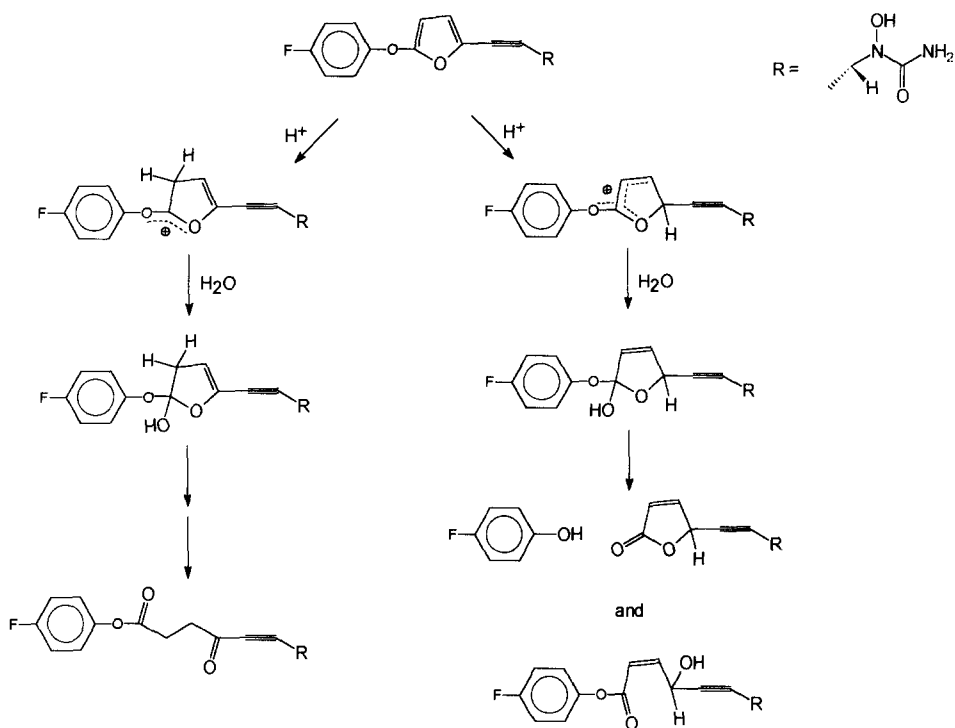


Fig. 7. One proposed mechanism for acidic hydrolysis of Abbott-79175.

zileuton studies was 0.2. The relative reactivity of Abbott-79175 compared to zileuton is directly related to the differences in substituents on these molecules. It is possible that in the acidic range the mechanism of degradation has changed compared to zileuton due to the substitution of the fluorophenoxyfuranylethyne for the benzothiofene of zileuton. Furans are known to be susceptible to acidic hydrolysis, which may be due to their lower resonance energy compared to other heterocycles like thiophene and pyrrole (March, 1977). For Abbott-79175, a substituted furan, a plausible reaction scheme involving the furan moiety in the acidic range, based on the work of Garst and Schmir (1974) with 2-methoxyfuran, is depicted in Fig. 7. This scenario would not be chemically reasonable for zileuton (structure of zileuton is shown in Fig. 8). Previous work by Kankaanpera and Aaltonen (1972) and by Garst and Schmir (1974) showed relatively rapid rates of hydrolysis of 2-methoxyfuran. Although Abbott-79175 possesses a more complicated structure than this model compound, the much greater

rate of acidic hydrolysis of Abbott-79175 vs zileuton can be explained based on the known lability to acidic hydrolysis by 2-alkoxy and presumably aryloxy furans. Due to the great qualitative similarity of the Abbott-79175 pH-rate profile in the neutral and alkaline ranges (although the rate is faster) to that of zileuton, a similar mechanism of degradation is believed to be operative. The rate disparity between Abbott-79175 and zileuton in neutral and alkaline solution may be attributed to differences in inductive effects of the substituents on their common hydroxyurea moiety. An examination of the degradation pathway of Abbott-79175, which is of considerable complexity, warrants a separate report.

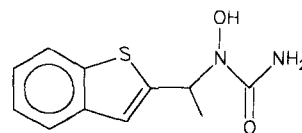


Fig. 8. Chemical structure of zileuton (Abbott-64077).

Table 5

Effect of ionic strength on rate of ionized Abbott-79175 degradation at 40°C

pH	$\mu$				
	0.1	0.2	0.3	0.4	0.5
12.89 <sup>a,b</sup>	0.137	0.120	0.118	0.137	0.122

<sup>a</sup> All apparent pseudo-first order rate constants are in  $\text{h}^{-1}$ .

<sup>b</sup> System consisted of 0.1 N NaOH with added NaCl to adjust  $\mu$ .

### 3.4. Effect of ionic strength

The rate of degradation of Abbott-79175 above its  $\text{p}K_a$  is unaffected by varying the ionic strength (Table 5). This further supports the absence of hydroxide ion participation in the rate-limiting step of Abbott-79175 anion degradation in aqueous solution. Although a similar study was not performed in the work of Alvarez and Slade (1992), the same independence of the reaction rate to hydroxide ion concentration, as demonstrated by the plateau of the rate profile in this region, was observed with zileuton and Abbott-79175.

### 3.5. Degradation rate temperature dependence

The relationship between the overall degradation rate constants ( $k_{\text{obs}}$ ) and temperature for those pH values studied is illustrated in Table 6. The differences in activation energies for Abbott-79175 at the various pH values (Table 7) indicate the change in mechanism of the reaction consistent with the kinetic model. The activation energies in the mildly to strongly alkaline regions are in the range of other urea-like compounds (Lynn, 1965; Vogels and Van der Drift, 1969; Welles et

Table 6

Abbott-79175 degradation rate constants as a function of temperature

pH	Temperature (°C)		
	40	60	70
2 <sup>a</sup>	1.49	4.42	7.06 <sup>b</sup>
4 <sup>a</sup>	0.03	0.13	0.24
5.99	0.006	0.030	0.076
8.06	0.005	0.05	0.19
10.09	0.10	0.80	1.87
12.03	0.11	1.49	3.12

<sup>a</sup> pH within 0.1 units of target value.

<sup>b</sup> All rate constants are expressed in  $\text{h}^{-1}$ .

al., 1971). Additional activation parameters for the  $k_{\text{obs}}$  in the various pH regions are also listed in Table 7. Enthalpy of activation which parallels the energy of activation is observed to increase with pH, as the entropic component becomes more positive. On entropic grounds alone, the degradation reaction in the acidic range would not be favored relative to reaction in the alkaline region (Moore and Pearson, 1981). However, this relatively unfavorable component (consistent with proton catalyst, water as a nucleophile, and drug molecule converging) is offset by the considerably reduced enthalpy of activation. It is important to note that the derived activation parameters are averages that are valid over the temperature range studied. This is primarily due to temperature effects on the complex ionic equilibria in solution.

## 4. Conclusions

Abbott-79175 has been shown to degrade according to pseudo-first order kinetics in the pH

Table 7

Activation parameters for  $k_{\text{obs}}$  at various pH values (40°C)

pH	$E_a$ (kcal/mol)	$\Delta H^\ddagger$ (kcal/mol)	$\Delta S^\ddagger$ (eu)	$\Delta G^\ddagger$ (kcal/mol)
2 <sup>a</sup>	11.1	10.5	-40.6	23.2
4 <sup>a</sup>	15.4	14.7	-34.9	25.7
5.99	17.8	17.2	-30.1	26.6
8.06	25.6	24.9	-5.7	26.7
10.09	20.6	20.0	-15.4	24.8
12.03	24.0	23.4	-4.4	24.8

<sup>a</sup> pH within 0.1 units of target value.

range from 1 to 13. It has been shown to be considerably more labile to specific acid catalysis than its predecessor zileuton and demonstrated a much narrower pH range of maximum stability than zileuton. Its qualitatively similar profile in the neutral and alkaline ranges suggests a similar mechanism for degradation in this region to zileuton. For both zileuton and Abbott-79175, it is abundantly clear that the rate-limiting component of the mechanism for degradation in the alkaline range does not include participation by hydroxide ion. Abbott-79175 has been shown to be susceptible to general acid/base catalysis which should be considered for any liquid formulation of this compound.

### Acknowledgements

The authors gratefully acknowledge the immunoscience venture for generously supplying Abbott-79175 for these studies, and thank Saul Borodkin, Kevin Garren and William Porter for reviewing the manuscript. The helpful discussions with Steven Krill are also acknowledged.

### References

- Alvarez, F.J. and Slade, R.T., Kinetics and mechanism of degradation of zileuton, a potent 5-lipoxygenase inhibitor. *Pharm. Res.*, 9 (1992) 1465–1473.
- Archer, D.W. and Monk, C.B., Ion-association constants of some acetates by pH (glass electrode) measurements. *J. Chem. Soc.*, (1964) 3117–3122.
- Bell, R.L., Brooks, D.W., Young, P.R., Lanni, C., Stewart, A.O., Bouska, J., Malo, P.E. and Carter, G.W., Abbott-78773: A selective, potent 5-lipoxygenase inhibitor. *J. Lipid Mediators*, 6 (1993) 259–264.
- Brooks, D.W., Summers, J.B., Gunn, B.P., Dellaria, J.F., Holms, J.H., Maki, R.G., Martin, J.G., Martin, M.B., Moore, J.L., Rodrigues, K.E., Stewart, A.O., Albert, D.H., Bell, R.L., Bouska, J.B., Dyer, R.D., Malo, P.E., Young, P.R., Rubin, P., Kesterson, J. and Carter, G.W., Abbott-64077, a promising therapeutic agent for treating leukotriene mediated diseases. *199th American Chemical Society Meeting*, Boston MA, April 22–27, 1990.
- Carter, G.W., Young, P.R., Albert, D.H., Bouska, J., Dyer, R., Bell, R.L., Summers, J.B. and Brooks, D.W., 5-Lipoxygenase Inhibitory Activity of Zileuton. *J. Pharmacol. Exp. Ther.*, 256 (1991) 929–937.
- Davies, C., *Ion Association*, Butterworth, Washington, DC, 1962.
- Flower, R.J., Moncada, S. and Vane, J.R., Analgesic-antipyretics and anti-inflammatory agents; Drugs employed in the treatment of gout. In Gilman, A.G., Goodman, L.S., Rall, T.W. and Murad, F. (Eds), *The Pharmacological Basis of Therapeutics*, Macmillan, New York, 1985, pp. 674–715.
- Garst, J.E. and Schmir, G.L., Hydrolysis of 2-methoxyfuran. *J. Org. Chem.*, 39 (1974) 2920–2923.
- Kankaanpera, A. and Aaltonen, R., General acid catalysis in the hydrolysis of a furan derivative. *Acta Chem. Scand.*, 26 (1972) 2537–2540.
- Lynn, K.R., Kinetics of base-catalyzed hydrolysis of urea. *J. Phys. Chem.*, 69 (1965) 687–689.
- March, J., *Advanced Organic Chemistry, Reactions, Mechanisms, and Structure*, 2nd Edn, McGraw-Hill, New York, 1977, p. 45, 346.
- Moncada, S., Flower, R.J. and Vane, J.R., Prostaglandins, prostacyclin, thromboxane A<sub>2</sub> and leukotrienes. In Gilman, A.G., Goodman, L.S., Rall, T.W. and Murad, F. (Eds), *The Pharmacological Basis of Therapeutics*, 7th Edn, Macmillan, New York, 1985, pp. 660–673.
- Moore, J.W. and Pearson, R.G., *Kinetics and Mechanism; A Study of Homogeneous Chemical Reactions*, 3rd Edn, Wiley, New York, 1981, pp. 179–181.
- Vogels, G.D. and Van der Drift, C., Hydrolysis of allantoate. *Recl. Trav. Chim. Pays-Bas*, 88 (1969) 951–957.
- Wasserman, M.A., Smith, E.F., Underwood, D.C. and Barrette, M.A., Pharmacology and pathophysiology of 5-lipoxygenase products. In Crooke, S.T. and Wong, A. (Eds), *Lipoxygenases and their Products*, Academic Press, San Diego, CA, 1991, pp. 1–50.
- Welles, H.L., Giaquinto, A.R. and Lindstrom, R.E., Degradation of urea in concentrated aqueous solution. *J. Pharm. Sci.*, 60 (1971) 1212–1216.